



## Modeling of velocity distributions of dust in tokamak edge plasmas and dust–wall collisions

R.D. Smirnov\*, S.I. Krasheninnikov, A.Yu. Pigarov<sup>1</sup>, D.J. Benson, M. Rosenberg, D.A. Mendis

University of California San Diego, 9500 Gilman Drive, La Jolla, CA 92093, USA

### ARTICLE INFO

PACS:  
52.55.Fa  
52.40.Hf  
52.25.Vy

### ABSTRACT

Velocity distribution functions of dust particles of various sizes are simulated in different regions of a tokamak using the DUSTT code. It is shown that dust particles accelerated by plasma flows can reach very high speed  $>1$  km/s at the terminal stages of vaporization. Collisions of beryllium and tungsten dust particles with beryllium wall are modeled with the LS-DYNA material structural analysis code. It is demonstrated that the collisions at high speed  $\sim 1$  km/s can cause significant damage to the wall or complete dust destruction depending on dust and wall material parameters.

© 2009 Elsevier B.V. All rights reserved.

### 1. Introduction

Much attention has been attracted recently to studying the behavior of microscopic dust particles and their impact on the performance of magnetic fusion devices. Dust can appear inside the main reactor chamber due to various surface damaging processes, such as wall material sputtering by plasma, flaking of deposited layers, melting, brittle destruction, arcing, etc., and due to impurity coagulation in cold contaminated plasma regions [1]. The interest in this subject is rising due to potential explosion and radiological hazards of dust accumulation in future reactors designed for ignited long pulse discharges. Dust is also associated with in-vessel tritium retention and impurity transport in edge plasmas. Moreover, it has been observed recently that burst production of dust due to intermittent high heat loads on plasma facing components may terminate long pulse discharges in LHD [2].

A number of theoretical and experimental studies of dust dynamics in edge plasmas of tokamaks were conducted recently, including observations and tracking of dust trajectories with fast cameras, and numerical simulations with the DUSTT code [3–5]. These studies are generally in agreement that a typical micron size dust particle in edge plasma can be accelerated by plasma flows to a characteristic speed of a few 100 m/s. However, recent analysis of probe data from the FTU tokamak suggests the presence of much faster particles with speed exceeding a few km/s. Such particles can produce spikes in the probe signal due to dust vaporization and ionization upon hypervelocity dust–probe collisions [6]. In this

paper we analyze dust particle velocity distribution functions (VDFs) in different regions of a tokamak for various dust sizes using DUSTT code simulations. The collisions of beryllium and tungsten dust with beryllium wall for different dust impact speeds are simulated using the material structural analysis code, LS-DYNA.

### 2. Modeling of dust velocity distribution functions with the DUSTT code

The DUSTT code [5,7], used recently to analyze and predict dust dynamics and transport in tokamak plasmas, allows the simulation of trajectories of individual dust particles in plasmas with known profiles, e.g. simulated with UEDGE code [8], as well as Monte-Carlo averaging of a large number of dust trajectories producing spatial profiles of averaged dust characteristics in such plasmas. The DUSTT code solves coupled equations of dust motion, charging, heating and ablation in time employing latest models of dust–plasma interaction processes. It takes into account acceleration of dust grains by ion drag, electrostatic, and gravity forces; charging of dust by plasma ions and electrons, as well as secondary electron and thermionic emissions; dust mass and energy balance due to absorption of plasma particles, ion surface recombination and thermal vaporization; physical and chemical sputtering of dust material, and radiation enhanced sublimation.

In this paper we employ the DUSTT code to simulate averaged local velocity distribution functions of carbon dust in three selected plasma regions in the inner and outer divertor, as well as in the outer midplane region of DIII-D tokamak. The DIII-D plasma parameters were calculated with the plasma transport code UEDGE. Dust particles of a fixed initial size are launched from all plasma exposed surfaces with initial speeds distributed according to a Maxwellian with thermal speed  $V_{d0} = 10$  m/s, and follow

\* Corresponding author.

E-mail addresses: [rsmirnov@ucsd.edu](mailto:rsmirnov@ucsd.edu) (R.D. Smirnov), [apigarov@ucsd.edu](mailto:apigarov@ucsd.edu) (A.Yu. Pigarov).

<sup>1</sup> Presenting author.

cosine angle distribution with respect to a local surface normal direction. Initial radius of dust particles,  $R_{d0}$ , is selected to be 0.1, 1.0, or 10.0  $\mu\text{m}$ . The injected flux of dust material corresponds to 1% of wall material locally sputtered by plasma. Under such assumption the divertor plates, which suffer from the largest plasma load due to recycling, are the main source of dust in the tokamak as was predicted in [9]. The amount of dust formed due to sputtering of first wall is much less than that of dust formed in the divertor despite the much larger area of the wall. In the present simulations dust material flux from divertor plates is  $4.54 \times 10^{18}$  atoms/s, while that from the wall is  $3.07 \times 10^{17}$  atoms/s. This consideration will be important for the following analysis of dust velocities.

The simulated distributions of dust particles' absolute speed, toroidal and poloidal velocities in the three selected plasma regions are shown in Fig. 1 for the three different initial radii of the particles  $R_{d0} = 0.1, 1.0,$  and  $10.0 \mu\text{m}$ . In the distributions shown the peak with near zero velocities corresponds to initial speeds of the injected dust particles. Following the injection the dust particles are accelerated by plasma flows mainly in the toroidal direction. The centrifugal force acting on such particles then accelerates them in the poloidal projection. It can be seen in Fig. 1 that there is an asymmetry of the dust toroidal velocity distributions in the inner and outer divertor regions due to the initial acceleration by plasma. Due to the opposite toroidal directions of plasma flows in the inner and outer divertor regions, the dust toroidal VDF in the inner divertor region is shifted largely in negative velocities, while in the outer divertor the velocities are shifted in the positive direction. Particles, penetrating from the inner divertor region into the outer one, form the negative part of the dust toroidal VDF there.

Besides the peak corresponding to initial dust velocities, there are other maxima in the dust VDFs at higher speeds correspond-

ing to the plasma accelerated particles. As particles get destroyed by plasma heating during motion and their radius,  $R_d$ , decreases, the plasma driven dust acceleration gets getting stronger, because the dust mass decreases as  $R_d^3$ , while the ion drag force is proportional to  $R_d^2$ . As we noted above, most of the simulated dust particles originate at the divertor plates. Depending on the distance of the plasma region, where the dust VDFs are analyzed, from the dust origin position, and on initial dust size the simulated VDFs have maxima at different values of dust speed. Also note, that there are two peaks corresponding to accelerated dust in the inner divertor region due to the shear structure of the plasma flows there. In the midplane region, dust particles do not reach such high speeds as in the divertor, because plasma flow velocities in the midplane are far less compared to the divertor region. Some very fast dust particles accelerated in the divertor can fly into the midplane region, but their number appears to be small.

In order to understand the dust VDFs simulated, we consider a simple one-dimensional model, where spherical dust particles move from a position of origin to a region of VDF measurements, while being continuously destroyed and accelerated by a uniform plasma. In such a model, the evolution of dust radius and speed are described by the following equations assuming dust thermal equilibrium

$$\frac{dR_d}{dt} = -\zeta_h \frac{nT^{3/2}m_a}{H_{vap}\rho m_i^{1/2}}, \quad \frac{dV_d}{dt} = \zeta_f \frac{nT}{R_d\rho}, \quad (1)$$

where  $R_d$  and  $V_d$  are the dust particle's radius and speed,  $n$  and  $T$  are the plasma density and temperature,  $\rho$  is the dust mass density,  $H_{vap}$  is the heat of vaporization (sublimation for carbon) per atom of dust material,  $m_i$  is the mass of a plasma ion,  $m_a$  is the mass of

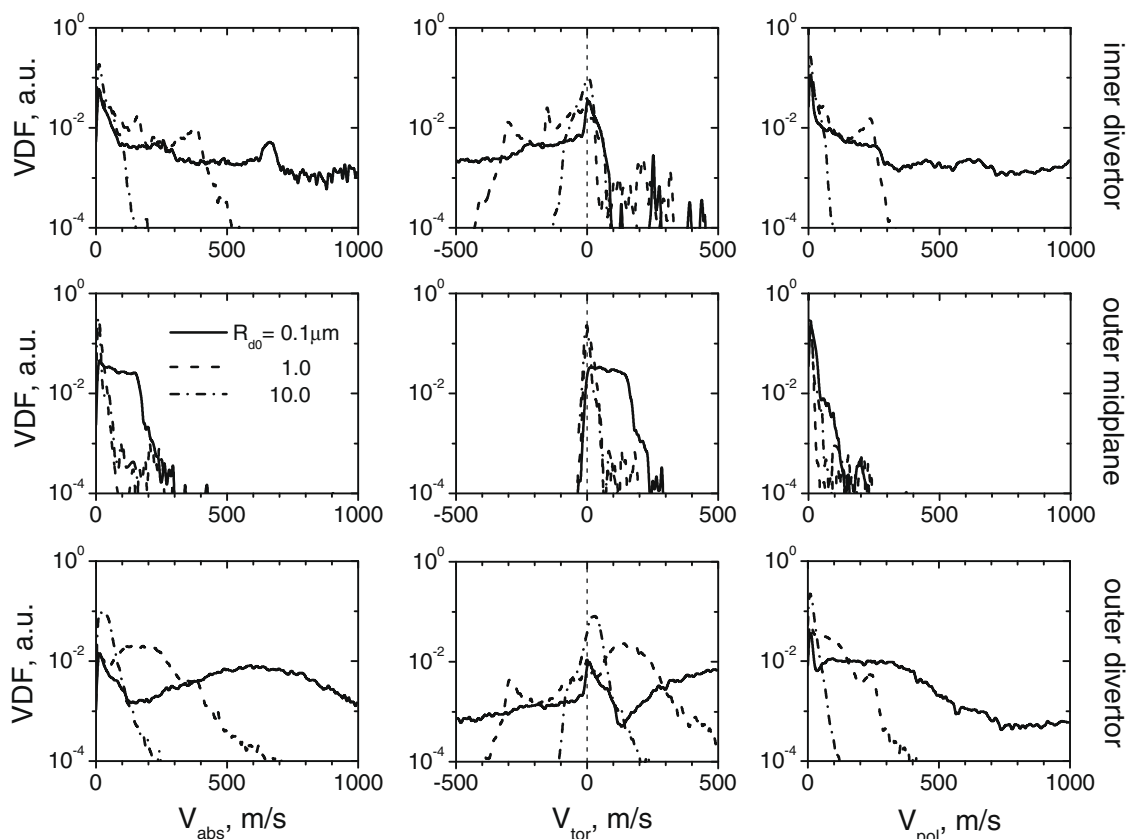


Fig. 1. Simulated distributions of dust absolute speed (left column), toroidal (middle column), and poloidal (right column) velocities in inner divertor (upper row), outer midplane (middle row), and outer divertor regions (bottom row) for different injected dust radii  $R_{d0} = 0.1, 1.0$  and  $10.0 \mu\text{m}$ .

a dust material atom, and  $\zeta_h$  and  $\zeta_f$  are numerical factors accounting for geometry in plasma heat and momentum flux to the dust particle, correspondingly. Eliminating time in Eq. (1) and solving them for the dust speed as function of the dust radius we obtain

$$V_d = V_{d0} + A \ln \left( \frac{R_{d0}}{R_d} \right), \quad A \equiv \frac{\zeta_f}{\zeta_h} \frac{H_{vap} m_i^{1/2}}{T^{1/2} m_a}, \quad (2)$$

where  $R_{d0}$  and  $V_{d0}$  are the dust initial radius and speed, correspondingly. For simplicity of further estimations we will assume  $V_{d0} = 0$ . Eq. (2) demonstrates a sharp increase of the accelerated dust particle's speed as its radius decreases. As one can see, Eq. (2) has a singularity, when  $R_d \rightarrow 0$ , that should be avoided by imposing a minimal dust radius, for which this model is applicable. Assuming that in this one-dimensional model the distance between the dust origin point and the diagnosed plasma region is  $L$ , after some algebra we obtain

$$\frac{1}{B} \frac{L}{R_{d0}} = 1 - \exp \left( -\frac{V_d}{A} \right) \left( 1 + \frac{V_d}{A} \right), \quad B \equiv \frac{\zeta_f}{\zeta_h^2} \frac{H_{vap}^2 \rho m_i}{n T^2 m_a^2}. \quad (3)$$

Using  $n = 10^{13} \text{ cm}^{-3}$ ,  $T = 10 \text{ eV}$ ,  $H_{vap} = 3 \text{ eV}$ ,  $\rho = 2 \text{ g/cm}^3$ ,  $m_i = 3.3 \times 10^{-24} \text{ g}$ ,  $m_a = 1.0 \times 10^{-23} \text{ g}$ ,  $\zeta_f \sim 10$ , and  $\zeta_h \sim 20$  for a carbon dust particle in deuterium plasma, we have  $A \sim 1000 \text{ m/s}$  and  $B \sim 1.5 \times 10^6$ . Note that value  $H_{vap} = 3 \text{ eV}$  used here takes into account sublimation of carbon by clusters at high temperatures. The dependence of the ratio  $L/(BR_{d0})$  on normalized dust speed  $V_d/A$  is plotted in Fig. 2. As follows from Eq. (3) and can be seen in Fig. 2, dust particle's speed is approximately proportional to  $\sqrt{L/R_{d0}}$  at selected location  $L$  from the dust source for particles with  $V_d < A$ . This is in accord with positions of maxima of the VDFs corresponding to the accelerated dust shown in Fig. 1, which scale with factor  $\sim 3$  in the velocity space, when the initial dust size changes by one order of magnitude. From Eq. (3) it follows that the dust particles cannot travel a distance larger than  $L_{max} = BR_{d0}$ , where they are completely destroyed. Fig. 2 shows also that the dust speed increases very sharply, when  $V_d > A$  and  $R_{d0} \sim L/B$ . This can explain the very long 'tails' of dust VDFs for small particles shown in Fig. 1, as even a small deviation in dust size and/or point of origin, always present in real conditions, leads to a large difference in dust speed. It also predicts that small particles can be accelerated to very high speeds  $> 1000 \text{ m/s}$  in edge plasmas of tokamaks.

### 3. Modeling of dust–wall collisions

As shown in Section 2, while most dust particles accelerated by tokamak plasmas acquire speeds of a few 100 m/s, some particles can reach very high speed  $\sim 1 \text{ km/s}$ . Such high speed particles colliding with the walls can be destroyed on the impact and/or cause substantial damage to the wall. To assess possible effects of dust–

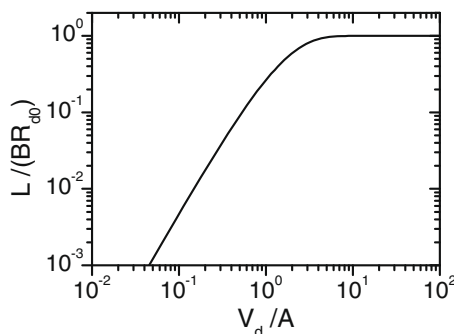


Fig. 2. Relation between dust speed  $V_d$  achievable by a dust particle at distance  $L$  from its point of origin and the particle's initial radius  $R_{d0}$  calculated using the simplified one-dimensional uniform plasma model.

wall collisions both on the dust and on the wall we performed numerical simulations using the commercial finite element code for structural analysis, LS-DYNA. The LS-DYNA code solves three-dimensional transient multi-physics problems including solid mechanics, deformation, contacts, fragmentation, heat transfer etc., and implements a large variety of material models and simulation techniques [10]. For the simulations of high velocity impact dynamics we employed Smoothed Particle Hydrodynamics (SPH) problem formulation, which allows the simulation of large deformations and fracturing of colliding bodies. Using this method we simulated impacts of  $0.5 \mu\text{m}$  beryllium and tungsten spherical dust particles on a flat beryllium target of  $6 \times 6 \times 3 \mu\text{m}$ , at the speeds 100 and 1000 m/s, and at the angle of  $45^\circ$  to the surface normal. The choice of dust/wall materials was suggested by relation to the ITER structural elements, as well as by the availability of data on material model parameters. We used Steinberg–Guinan material model for the metals of choice, as it is applicable for simulation of plastic deformations with very high strain rates [11]. The modeled values of yield strength of beryllium and tungsten are  $Y_{Be} = 0.33 \text{ GPa}$ ,  $Y_W = 2.2 \text{ GPa}$ , and the ultimate strength on compression  $G_{Be} = 1.31 \text{ GPa}$  and  $G_W = 4.0 \text{ GPa}$ , correspondingly. In the present simulations we neglected thermal effects, assuming constant temperature of the dust and the target set at 500 K. No external forces were present in the simulations, such as electric force, as their work on the simulated length scale is negligible in comparison with the dust kinetic energy.

The results of the simulations of the dust–wall collisions are shown in Fig. 3. A beryllium dust particle at low speed 100 m/s causes no significant damage to the wall, being reflected from the wall, partially deformed and destroyed due to shear stresses developed during the oblique collision, Fig. 3(a). It is noted that the particle starts spinning after the reflection with estimated angular speed  $\sim 10^7 \text{ s}^{-1}$ . At high impact speed of 1 km/s beryllium dust is completely destroyed upon collision with the wall, forming a cone of debris material injected into the plasma, Fig. 3(b). At the low speed of 100 m/s the tungsten dust causes noticeable damage to the wall, ejecting into the plasma about the same amount of fractured wall material as the dust volume, Fig. 3(c). The tungsten particle itself remains in good shape, with insignificant deformation. At the high speed of 1000 m/s, the tungsten dust causes significant wall damage forming a large crater at the target surface. The remains of the destroyed particle can be found at the bottom

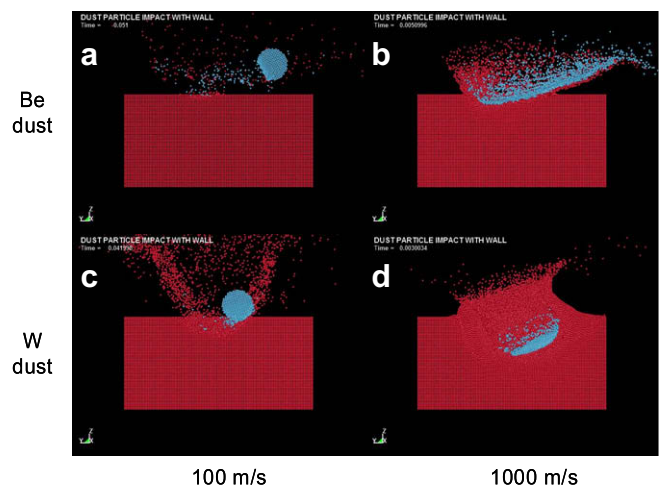


Fig. 3. Simulated impact of beryllium and tungsten dust particles of  $0.5 \mu\text{m}$  radius (blue) on beryllium target (red) at speeds 100 and 1000 m/s, and impact angle of  $45^\circ$ . (For interpretation of the references to color in this figure legend, the reader is referred to the web version of this article.)

of the crater. We suspect that such dust, impacting on re-deposited layers or rough wall surfaces, may lead to significant secondary dust production. Let us note that the simulated high velocity dust impact with speed 1000 m/s is still below the hypervelocity threshold, which requires impact speed exceeding velocity of compressive shock wave propagating in the target.

#### 4. Summary

In this work the dust velocity distribution functions at different locations of DIII-D tokamak were analyzed for various dust radii using DUSTT code simulations and theoretical estimations. It was shown that small dust particles and particles at terminal vaporization stages can be accelerated by plasma flows to very high speed  $>1$  km/s. The velocity corresponding to the maximum of the dust VDF at a given distance  $L$  from the location of dust origin is shown to be approximately proportional to  $\sqrt{L/R_{d0}}$ , where  $R_{d0}$  is the initial radius of dust particles. The collisions of beryllium and tungsten dust particles with a beryllium wall at 100 and 1000 m/s impact speeds were simulated. It was demonstrated that the high speed impact can cause significant damage to the wall and/or complete destruction of the dust particle upon collision, depending on the relative strength and mass density of the dust and wall materials. These effects can be important for describing dust transport in

tokamaks, and can present potentially important wall damaging mechanism. We plan further simulations of dust-wall collisions including rough and overcoated surfaces to investigate possible mechanisms of secondary dust production and to obtain dust-wall impact parameters, such as coefficients of restitution and rebound angle distributions, for more realistic input into dust-wall collision models used in the DUSTT code.

#### Acknowledgements

This work was supported in part by the US DoE under Grant DE-FG02-04ER54852.

#### References

- [1] J. Winter, Plasma Phys. Control. Fus. 40 (1998) 1201.
- [2] K. Saito et al., J. Nucl. Mater. 363–365 (2007) 1323.
- [3] A.L. Roquemore et al., J. Nucl. Mater. 363–365 (2007) 222.
- [4] D.L. Rudakov et al., J. Nucl. Mater. 363–365 (2007) 227.
- [5] R.D. Smirnov et al., Plasma Phys. Control. Fus. 49 (2007) 347.
- [6] C. Castaldo et al., Nucl. Fus. 47 (2007) L5.
- [7] A.Yu. Pigarov et al., Phys. Plasmas 12 (2005) 122508.
- [8] T.D. Rognlien et al., J. Nucl. Mater. 196 (1992) 347.
- [9] S.I. Krashenninnikov et al., Phys. Plasmas 11 (2004) 3141.
- [10] <http://www.lstc.com/lstdyna.htm>.
- [11] D.J. Steinberg et al., J. Appl. Phys. 51 (1980) 1498.